Physics and Chemistry of the Earth 128 (2022) 103288

Contents lists available at ScienceDirect

Physics and Chemistry of the Earth

journal homepage: www.elsevier.com/locate/pce

Modeling COVID-19 infection in high-risk settings and low-risk settings

Meshach Ndlovu *, Mqhelewenkosi A. Mpofu, Rodwell G. Moyo

Gwanda State University Department of Geomatics and Surveying, Zimbabwe

ARTICLE INFO

Keywords:
COVID-19
Risk settings
Alternating risk levels
Population dynamics

ABSTRACT

In this research paper we present a mathematical model for COVID-19 in high-risk settings and low-risk settings which might be infection dynamics between hotspots and less risky communities. The main idea was to couple the SIR model with alternating risk levels from the two different settings high and low-risk settings. Therefore, building from this model we partition the infected class into two categories, the symptomatic and the asymptomatic. Using this approach we simulated COVID-19 dynamics in low and high-risk settings with auto-switching risk settings. Again, the model was analyzed using both analytic methods and numerical methods. The results of this study suggest that switching risk levels in different settings plays a pivotal role in COVID-19 progression dynamics. Hence, population reaction time to adhere to preventative measures and interventions ought to be implemented with flash speed targeting first the high-risk setting while containing the dynamics in low-risk settings.

1. Introduction

COVID-19 disease is defined as the disease caused by SARS-CoV-2, the coronavirus that emerged in December 2019 (Zhu et al., 2020). This disease originated in Wuhan province, Wuhan in China by the close of the year 2019 (Anon, 2020). Following this major outbreak, the disease then spread to different countries, and continents and Zimbabwe recorded its first case by the end of March 2020. The disease first spread to major cities like Harare, Bulawayo, and Victoria Falls and it later spread to other cities and rural areas. The spread of this disease within the country lead to a series of intervention measures for example lockdowns, social distancing, and disinfection of public places. According to World Health Organization (WHO) reports, Zimbabwe had recorded more than 121 000 cases including 4 156 deaths by August 2021 (Zhu et al., 2020; Anon, 2020).

The major signs and symptoms of this disease include severe pneumonia, low respiratory airways, fatigue, headache, loss of taste or smell, and sore throat (Volpicelli and Gargani, 2020; Rali and Sauer, 2020). The disease is mainly spread through contact with infected people or through contact with contaminated surfaces. When a susceptible individual is exposed to the virus, symptoms may appear after 2–14 days and the patient may die or recover in 2 weeks. An infected person may be either symptomatic or asymptomatic but they are all infectious. An asymptomatic patient may spread the disease more than a symptomatic patient since individuals may not be aware of their sickness unless tested (Kumar, 2020).

COVID-19 may be transmitted through respiratory droplets which can travel a distance of six feet or less in the air. It may also be transmitted through fomites (indirectly) for the time the virus is on the environmental surfaces and the time may range from hours to days. For the transmission process to take, the contaminated droplets need reach to the eyes, nose, or mouth of a susceptible individual (Galbadage and Peterson, 2020; Xiang et al., 2020).

The spread of SARS-CoV-2 can be prevented through exercising high levels of cleanliness. Frequent washing of hands with soap or hand sanitizer, proper wearing of face masks, and practicing social distancing can help reduce the spread of this deadly disease. Most importantly, it is encouraged individuals should stay at home and avoid unnecessary movements and mixing with people. Strict COVID-19 lockdown measures have been put in place by the government of Zimbabwe in order to help stop its spread. Public service offices were de-congested, the workforce reduced in different companies, and inter-city travel banned (during level 4 of lockdown) (Mackworth-Young et al., 2021). The country had to also welcome the administration of the COVID-19 vaccine, Sinovac and Sinopharm were developed in China. Despite all these measures, covid-19 has remained a major challenge in the country, especially in large cities like Harare and Bulawayo as they recorded high numbers of cases per day (Murewanhema and Makurumidze, 2020; Dzinamarira et al., 2021).

Harare and Bulawayo are the largest cities in Zimbabwe characterized by large populations, with Harare being the highest followed

* Corresponding author.
E-mail address: meshach.ndlovu@gsu.ac.zw (M. Ndlovu).

https://doi.org/10.1016/j.pce.2022.103288
Received 17 October 2021; Received in revised form 13 September 2022; Accepted 20 October 2022
Available online 2 November 2022

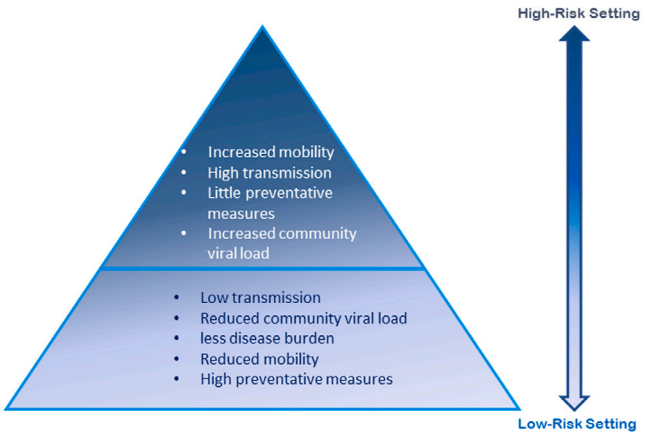

Fig. 1. Risk Setting Pyramid.

by Bulawayo. According to the 2012 census, Harare province had a population of more than 2.4 million while Bulawayo province recorded a population of about 665,940 (Anon, 2022). Whenever there was a disease outbreak, these and other big cities of Zimbabwe were the first ones to be affected. Communicable diseases like Covid-19 spread at a fast rate in such areas and they may be said to be high-risk areas (Mackworth-Young et al., 2021; Murewanhema and Makurumidze, 2020; Dzinamarira et al., 2021). With respect to Covid-19, high-risk areas are associated with high infection rates, infectious Covid-19 variants like 'Beta' and the environmental viral load is high (Brindle and Gawande, 2020). Rural areas and other less populated areas may be referred to as low-risk areas as far as Covid-19 is concerned. These areas are characterized by low mobility (reducing chances of importing the disease) and low infection rate, few reported cases, less infectious variants like Alpha' and the environmental viral load is very low.

1.1. High-risk setting and low-risk setting

In this section, we present a risk-setting pyramid with two levels at the bottom is a low-risk setting, and at the top is a high-risk setting (see Fig. 1).

A high-risk setting can be viewed in 2-dimension firstly the higher risk of developing critical illness due to the disease, secondly, the high-risk setting as a population with a high transmission rate of increased community viral load, increased mobility, and population with few preventative measures in place. The first case of higher-risk groups involves individuals with the following chronic conditions asthma, diabetes, lung disease, obesity, sickle cell disease, and heart disease which increase the severity of Covid-19 amongst the infected individual. This study focuses on the high-risk setting in the context of increased transmission rate together with high mobility as factors impacting the rapid propagation of the disease.

Adherence to Covid-19 preventative measures has a positive influence on the risk levels of the population the higher the adherence to the preventative measures the lower the risk of contracting the disease. On the other hand, the lower adherence to Covid 19 preventative measures the higher the risk of contracting the disease. Therefore, hand washing, wearing of a mask in public spaces, quarantine, social distancing, proper building ventilation, and vaccinations are some of the preventative measures installed by the populations to minimize the risk of the disease.

In a low-risk setting there exist a low transmission rate, reduced community viral load i.e an environment with few reservoirs or sources of the disease, less disease burden, reduced mobility i.e low risk of importing new infections, and high adherence to preventative measures. The use of clinical datasets has played a pivotal role in making recommendations on certain preventative methods that can impact the Covid-19 community levels. Through the use of baseline data communities/populations can then be classified as either high-risk settings or low-risk settings.

2. Model formulation

A mathematical model is defined as a description of a real-life situation in mathematics terms. Hence, so far scientists have developed many mathematical models to represent the dynamics of Covid-19 for example (Li et al., 2020; Riou and Althaus, 2020; Zhong et al., 2021; Zhou et al., 2020). In this study, we extend a basic SIR model to model a Covid-19 infection in high and low-risk settings (Weiss, 2013). The model is in the form of eight ordinary differential equations which shows how the members in a 'Covid-19 present environment' interact as time progresses. The total human population has been divided into eight compartments.

The susceptible population has been divided into two classes, the susceptible from a low risk, S_L and the susceptible from high risk, S_H. Infected individuals are not always symptomatic, some are asymptomatic and do not show any signs and symptoms of infection. The total number of infected individuals has been grouped into four classes, Infected symptomatic from a low-risk setting (I_{SL}), Infected asymptomatic from a low risk (I_{AL}), infected symptomatic from a high-risk setting (I_{SH}) and infected asymptomatic from a high-risk setting (I_{AL}). The last two compartments are for the recovered individuals, the first being the recovered from a low-risk setting and the recovered from a high risk. Members are added to the susceptible classes at a rate of θ. μS_L and μS_H represent the natural death rate in low and high-risk settings respectively. Members are removed from the susceptible low risk to the Infected symptomatic low risk and infected asymptomatic low risk respectively by $(1-\pi_1)\beta S_L I_{\mathrm{SL}}$ and $\pi_1\beta S_L I_{\mathrm{AL}}$. On a high risk setting the, the rate of moving from the susceptible population to the infected symptomatic and infected asymptomatic is respectively given by $(1-\pi_2)\beta S_H I_{\mathrm{SH}}$ and $\pi_2\beta S_H I_{\mathrm{AH}}$. The susceptible low-risk interact with the infected asymptomatic at a rate of $\pi_4\beta S_L I_{\mathrm{AH}}$ and the susceptible high-risk move to the infected asymptomatic low-risk class at a rate of $\pi_3\beta S_H I_{\mathrm{AL}}$. The model assumes that there is no interaction between the infected symptomatic and other classes. The disease-induced death for symptomatic low-risk and asymptomatic low risk is given by αI_{SL} and ϕI_{AL} respectively. In a high-risk setting, infected symptomatic die at a rate of αI_{SH} and ϕI_{AH} is the number of deaths of the asymptomatic. The infected asymptomatic classes for both settings can interact. $\tau_2 I_{\mathrm{AL}}$ is the rate of moving from the infected asymptomatic low risk to the infected asymptomatic and $\tau_1 I_{\mathrm{AH}}$ for the vice-versa. After some time, infected individuals are removed from the infected class to the recovered by κI_{SL} and σI_{AL} in a low risk setting and by κI_{SH} and σI_{AH} in a high risk setting. After recovering from the disease, members from a low and high risk may face natural death at a rate of μR_L and μR_H respectively.

2.1. Compartmental model

Fig. 2 gives a photographic view of our model. We see a visual description of how the susceptible class for both the low and high-risk settings progresses in the respective infectious classes and later progresses into the recovery classes. From Fig. 2 the arrows depict the possible movements of individuals from one compartment to the other at a given rate as labeled in the diagram. The interaction between the infectious compartment at low risk and that at high-risk settings may be caused by the migration of individuals from a low-risk environment to a high-risk environment and vice versa. This may be possible only for the asymptomatic infectious group as they can move around easily without the virus being detected. However, the is no flow between broken lines but these represent the possibility of interaction of individuals from the two-compartment without necessarily moving individuals.

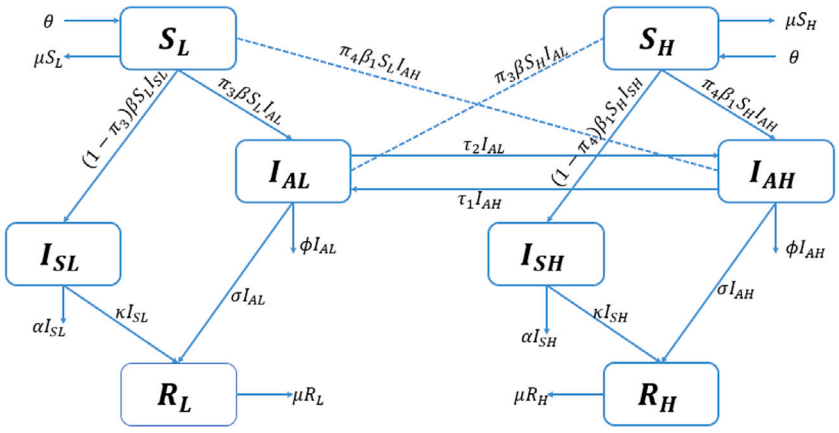

Fig. 2. Deterministic Model a pictorial view of high and low-risk settings dynamics.

The compartmental model is the pictorial view of the network flow and shows how these eight compartments (classes) are interlinked. An individual can progress from one compartment to another. Therefore, this general mathematical modeling tool has great power in the development of simulation schemes that can be used by decision-makers. Many biological systems or dynamic systems phenomena when compared to these models provide the validity and applicability of this kind of research tool. Compartmental models help to predict the current future trends of systems or diseases. A mathematical model can then be used to test different types of intervention measures that may contribute to different directions of the disease during a pandemic. Hence, this is the main reason why compartmental models are useful in disease modeling and epidemiology.

From Fig. 2, we obtain the following systems of ordinary differential equations.

$$\begin{aligned}
\frac{dS_L}{dt} &= \theta - \mu S_L - (1-\pi_3)\beta S_L I_{SL} - \pi_3 \beta S_L I_{AL} - \pi_4 \beta_1 S_L I_{AH} \\
\frac{dS_H}{dt} &= \theta - \mu S_H - (1-\pi_4)\beta_1 S_H I_{SH} - \pi_4 \beta_1 S_H I_{AH} - \pi_3 \beta S_H I_{AL} \\
\frac{dI_{AL}}{dt} &= \pi_3 \beta S_L I_{AL} + \pi_3 \beta S_H I_{AL} + \tau_1 I_{AH} - (\tau_2 + \phi + \sigma) I_{AL} \\
\frac{dI_{AH}}{dt} &= \pi_4 \beta_1 S_H I_{AH} + \pi_4 \beta_1 S_L I_{AH} + \tau_2 I_{AL} - (\tau_1 + \phi + \sigma) I_{AH} \\
\frac{dI_{SL}}{dt} &= (1-\pi_3)\beta S_L I_{SL} - (\alpha + \kappa) I_{SL} \\
\frac{dI_{SH}}{dt} &= (1-\pi_4)\beta_1 S_H I_{SH} - (\alpha + \kappa) I_{SH} \\
\frac{dR_L}{dt} &= \kappa I_{SL} + \sigma I_{AL} - \mu R_L \\
\frac{dR_H}{dt} &= \kappa I_{SH} + \sigma I_{AH} - \mu R_H
\end{aligned} \tag{1}$$

The model of differential equations can be analyzed qualitatively and quantitatively. In performing qualitative analysis the following calculations were conducted including equilibrium points, reproduction number, and sensitivity analysis. On the other hand, the quantitative analysis includes performing numerical simulations.

2.2. Transmission rate

A transmission rate is the measure of the spread of disease in a population. As discussed in the following papers (Zhu et al., 2020; Anon, 2020; Li et al., 2020; Riou and Althaus, 2020; He et al., 2013; Lin et al., 2020) Covid-19 transmission is the spread of the virus in the community through different mediums. The first case of consideration in this study is the case constant transmission rate shown in Fig. 3 which is our control.

Fig. 3 shows a constant transmission rate β for population B in a low-risk setting for all the time intervals $0 < t < 20$ and $t \geq 20$. Again,

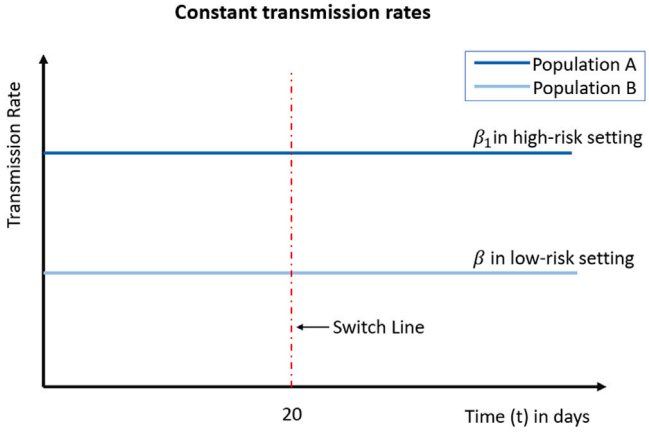

Fig. 3. Two populations, population A and population B with constant risk settings.

for population A the transmission rate β_1 was maintained at the same level for all the time intervals $0 < t < 20$ and $t \geq 20$. The switch line at $t = 20$ or simply the switch point represents the duration for the public to react in Covid-19 settings. The value of 20 is assumed since it falls within the duration range for public reaction cited by Mushayabasa et al. (2020) in He et al. (2013), Lin et al. (2020). However, is an arbitrary point in the study to effect a switch from one risk setting to the other for a population as highlighted in Fig. 4.

The second case of consideration is the out-of-control scenario with switching transmission rates from one risk setting to another. Therefore, by making an assumption that this jump happens at a point $t = 20$. According to Fig. 4, the population B starts with constant transmission rate β in a low-risk setting for the time interval $0 < t < 20$ and then switch at the switch line to a transmission rate β_1 in high-risk setting for the time interval $t \geq 20$.

For population A it launches at a high-risk setting with transmission rate β_1 on the interval $0 < t < 20$ but switches to a low-risk setting on the interval $t \geq 20$ with transmission rate β. The purpose of switching transmission rates is due to the seasonality attribute of Covid-19 (Ndlovu et al., 2022) and evidence of the multiscale nature of infectious diseases (Garira, 2018; Garira et al., 2014). Thus, the mathematical equations derived from Fig. 4 are as follows:

$$\text{Transmission on Population A} = \begin{cases} \beta_1 & 0 < t < 20 \\ \beta & t \geq 0 \end{cases} \tag{2}$$

$$\text{Transmission on Population B} = \begin{cases} \beta & 0 < t < 20 \\ \beta_1 & t \geq 0 \end{cases} \tag{3}$$

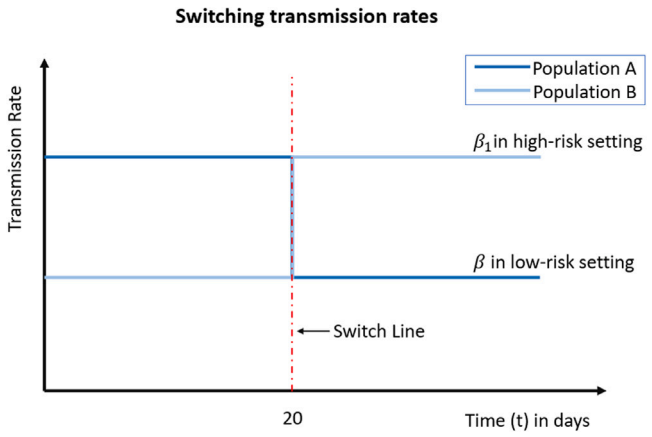

Fig. 4. Two populations, population A and population B with switching risk settings.

Eqs. (2) and (3) are piecewise functions used for mathematical modeling of the population switch from one risk setting to another.

3. Analysis of the model.

In the preliminary stages of the analysis of the model, we determined the disease equilibrium points and also computed the reproduction number R_0, which serves as pointers to the model Eq. (1). The qualitative analysis will highlight critical insights into the validity, reliability, and behavior of the dynamical system model.

3.1. Disease free equilibrium point

A disease-free equilibrium point E^* exists when the system of ordinary differential equations (1) is equated to zero to obtain the following solutions;

$$\begin{bmatrix} S_L^* \\ S_H^* \\ I_{AL}^* \\ I_{AH}^* \\ I_{SL}^* \\ I_{SH}^* \\ R_L^* \\ R_H^* \end{bmatrix} = \begin{bmatrix} \frac{\theta}{\mu} \\ \frac{\theta}{\mu} \\ 0 \\ 0 \\ 0 \\ 0 \\ 0 \\ 0 \end{bmatrix} \tag{4}$$

On the other hand, the equilibrium point can be viewed as the kernel of the system Eq. (1), and under these conditions, the virus is not expected to exist in the population. Again the system is stable at the equilibrium point.

3.2. Reproduction number (R_0)

The basic reproduction number is defined as the disease's potential to spread within a given population. It may also be defined as a metric that is used to describe the ability of transmission by infectious agents. It is the number of secondary cases from an infectious individual in his/her entire infectious period. In this model, we calculated our reproduction numbers for the low and high-risk settings using the next-generation matrix. The basic reproductive number is used to determine the local stability of the disease-free equilibrium point. The disease-free equilibrium point is locally stable when $R_0 < 1$ and unstable whenever $R_0 > 1$.

For a low-risk setting, the basic reproduction number is given as

$$R_L = \frac{2\beta\theta\pi_1}{\mu(\tau_2 + \sigma + \phi)} \tag{5}$$

For a high-risk setting, the basic reproductive number is given by

$$R_H = \frac{2\beta_1\theta\pi_2}{\mu(\tau_1 + \sigma + \phi)} \tag{6}$$

Each environment, community, and population either low-risk or high-risk has its own specific reproduction number since the infectious individuals from the different settings have a different average rate of spreading the infection.

3.3. Stability analysis

The local stability of the disease-free equilibrium point was obtained by examining the linearized form of the system at the steady state E^*. See Eq. (7) given in Box I, where $\omega_2 = -\tau_2 - \phi - \sigma - \mu$, $\omega_0 = -\tau_1 - \phi - \sigma - \mu$ and $\omega_1 = -\alpha - \kappa - \mu$. The local stability is investigated using the Jacobian matrix $J(E^*)$ eigenvalues. The disease-free equilibrium point E^* is said to be locally asymptotically stable if the real parts of the eigenvalues are all negative, otherwise, it is said to be unstable. The computed eigenvalues were: $\lambda_1 = -\mu$, $\lambda_2 = -\mu$, $\lambda_3 = -\mu$, $\lambda_4 = -\mu$,

$\lambda_5 = \frac{-\pi_3\beta\theta + \beta\theta + \mu\omega_1}{\mu}$, $\lambda_6 = \frac{\beta_1\theta - \pi_4\beta_1\theta + \mu\omega_1}{\mu}$, see $\lambda_{7,8}$ in Box II. The first four eigenvalues $\lambda_1\lambda_4$ are clearly negative whereas conditions for λ_5, λ_6 are $\beta\theta + \mu\omega_1 < \pi_3\beta\theta$ and $\beta_1\theta + \mu\omega_1 < \pi_4\beta_1\theta$ respectively. In the case of $\lambda_{7,8}$ the first should satisfy the following condition $2\pi_4\beta_1\theta + 2\pi_3\beta\theta < -\mu\omega_0 - \mu\omega_2$. For $\tau_2 < \tau_1$, $\beta_1 > \beta$, and $\pi_4 > \pi_3$ and applying these conditions we observe that $\omega_0 > \omega_2$ together with $2\pi_4\beta_1 > 4\pi_3\beta$ hence the discriminant of the eigenvalues is always positive subject to governing conditions. Therefore, the disease-free equilibrium is locally asymptotically stable when $R_0 < 1$. Thus, when $\max\{R_H, R_L\} < 1$ is in the close neighborhood of zero by manifold analysis. Hence, the disease-free equilibrium is locally asymptotically stable when $\max\{R_H, R_L\} < 1$.

3.4. Sensitivity analysis of (R_0)

The effect of each parameter in the spread of the infection was analyzed using sensitivity analysis of R_0. We differentiated R_L and R_H with respect to each parameter in Eqs. (5)–(6) and observed whether the parameters had a positive index or a negative index.

$$\begin{aligned}
\frac{d}{d\theta}(R_L) &= \frac{2\beta\pi_1}{\mu(\tau_2 + \sigma + \phi)} > 0 \\
\frac{d}{d\beta}(R_L) &= \frac{2\theta\pi_1}{\mu(\tau_2 + \sigma + \phi)} > 0 \\
\frac{d}{d\pi_1}(R_L) &= \frac{2\beta\theta}{\mu(\tau_2 + \sigma + \phi)} > 0 \\
\frac{d}{d\mu}(R_L) &= \frac{-2\beta\theta\pi_1}{\mu^2(\tau_2 + \sigma + \phi)} < 0 \\
\frac{d}{d\tau_2}(R_L) &= \frac{-2\beta\theta\pi_1}{\mu(\tau_2 + \sigma + \phi)^2} < 0 \\
\frac{d}{d\sigma}(R_L) &= \frac{-2\beta\theta\pi_1}{\mu(\tau_2 + \sigma + \phi)^2} < 0 \\
\frac{d}{d\phi}(R_L) &= \frac{-2\beta\theta\pi_1}{\mu(\tau_2 + \sigma + \phi)^2} < 0 \\
\frac{d}{d\pi_2}(R_H) &= \frac{2\beta_1\theta}{\mu(\tau_1 + \sigma + \phi)} > 0 \\
\frac{d}{d\tau_1}(R_H) &= \frac{-2\beta_1\theta\pi_2}{\mu(\tau_1 + \sigma + \phi)^2} < 0
\end{aligned} \tag{8}$$

From equations in (8), the following parameter set contains $\{\theta, \beta, \mu, \sigma, \phi, \pi_1, \pi_2, \tau_1, \tau_2\}$ and $\{\mu, \sigma, \phi, \tau_1, \tau_2\}$ have a negative index meaning that in order for us to reduce R_0, we need to work on reducing parameters with a negative index. Since we cannot control the natural death rate, we then need to influence or work on reducing disease-induced death reduces the movement of individuals from low-risk settings to high-risk settings.

$$J(E^*) = \begin{pmatrix} -\mu & 0 & -\frac{\beta\theta\pi_3}{\mu} & -\frac{\theta\pi_4\beta_1}{\mu} & -\frac{\beta\theta(1-\pi_3)}{\mu} & 0 & 0 & 0 \\ 0 & -\mu & -\frac{\beta\theta\pi_3}{\mu} & -\frac{\theta\pi_4\beta_1}{\mu} & 0 & -\frac{\theta(1-\pi_4)\beta_1}{\mu} & 0 & 0 \\ 0 & 0 & \frac{2\beta\theta\pi_3}{\mu} + \omega_2 & \tau_1 & 0 & 0 & 0 & 0 \\ 0 & 0 & \tau_2 & \frac{2\theta\pi_4\beta_1}{\mu} + \omega_0 & 0 & 0 & 0 & 0 \\ 0 & 0 & 0 & 0 & \frac{\beta\theta(1-\pi_3)}{\mu} + \omega_1 & 0 & 0 & 0 \\ 0 & 0 & 0 & 0 & 0 & \frac{\theta(1-\pi_4)\beta_1}{\mu} + \omega_1 & 0 & 0 \\ 0 & 0 & \sigma & 0 & \kappa & 0 & -\mu & 0 \\ 0 & 0 & 0 & \sigma & 0 & \kappa & 0 & -\mu \end{pmatrix} \tag{7}$$

Box I.

$$\lambda_{7,8} = \frac{2\pi_4\beta_1\theta + 2\pi_3\beta\theta + \mu\omega_0 + \mu\omega_2}{2\mu} \pm \frac{\sqrt{\left(2\pi_4\beta_1\theta + \mu\left(\omega_0 - \omega_2\right)\right)\left(2\pi_4\beta_1\theta - 4\pi_3\beta\theta + \mu\omega_0 - \mu\omega_2\right) + 4\left(\pi_3^2\beta\theta^2 + \mu^2\tau_1\tau_2\right)}}{2\mu}$$

Box II.

Table 1
Model parameter values and their description.

Parameter	Description
μ	Natural death rate
θ	Natural birth rate
β	Infection rate
π_1	Modifying factor on asymptomatic low-risk
π_2	Modifying factor on asymptomatic high-risk
π_3	Modifying factor on symptomatic high-risk
π_4	Modifying factor on symptomatic low-risk
α	Disease induced death rate of Infected symptomatic
ϕ	Disease induced death of infected asymptomatic
κ	Recovery rate of infected symptomatic
σ	Recovery rate of infected asymptomatic
τ_1	Movement rate from I_{AH} to I_{AL}
τ_2	Movement rate from I_{AL} to I_{AH}

Table 2
Table with model parameters values.

Parameter	Value	Source
μ	0.0342	Mushayi et al. (2021)
θ	0.0342	Mushayi et al. (2021)
β	[0.183–0.524]	Fitted
π_1	0.15	Estimated
π_2	0.15	Estimated
π_3	0.85	Estimated
π_4	0.85	Estimated
α	[0.0384–0.0611]	Mushayabasa et al. (2020)
ϕ	[0.0384–0.0611]	Mushayabasa et al. (2020)
κ	[0,2862–0.5231]	Mushayabasa et al. (2020)
σ	[0,2862–0.5231]	Mushayabasa et al. (2020)
τ_1	0.15	Estimated
τ_2	0.25	Estimated

4. Numerical simulations

In this section we present results from the simulation of the system of ordinary differential equations (1). Running numerical simulation aid in understanding the behavior of the population subjected to different parameter values. Furthermore, the numerical simulations will assist in exploring the dynamics of the complex system with advantages as compared to the analytic solutions. The parameter description used were summarized and given in Table 1.

Table 1 shows the model parameters and what they represent and again Table 1 helps regulate the model since the parameters have been described. The parameter values in Table 2 were mainly obtained from previous authors, some were fitted into the model while others were estimated. These estimated parameters were varied so as to understand the model behavior. Parameter values together with parameters description are the main ingredients for model calibration. Hence, the output values of the variables are dependent on the assigned parameter values.

To control the behavior of the model some parameters which include transmission rate β, the disease-induced death rate of infected symptomatic α, the disease-induced death rate of infected asymptomatic ϕ, the recovery rate of infected symptomatic κ, and the recovery rate of infected asymptomatic σ were assigned specific range on values. The transmission rate at the low-risk setting was considered to be 0.183 and the transmission rate at the high-risk setting was considered to be 0.524. Thus, to obtain the estimated value approximate judgment approach was applied together with the numerical simulations.

The information presented in Tables 1 and 2 supports the exploration of the numerical behavior of the system. Also, this information was foundational in formulating model adjustments. In the next section, we compare run and compare numerical simulations for two cases of low and high-risk settings with constant respective transmission rates, and low and high-risk settings with switching transmission rates.

4.1. Case 1: High and low-risk settings

In this section we present the simulation graphs obtained that demonstrate the behavior of the disease in low-risk setting and high-risk settings. The influence of the disease is observed in the basic model (model without modifications). Therefore, we present three diagrams (i) population dynamics in low-risk setting control, (ii) population dynamics in high-risk setting control, and (iii) infected population dynamics in both low-risk settings and high-risk settings.

Fig. 5 shows the dynamics of this disease in a low-risk setting. The dynamics show the behavior of the three classes, Susceptible, infected symptomatic, and infected asymptomatic. The susceptible population initially rises rapidly but decreases as soon as the infected population

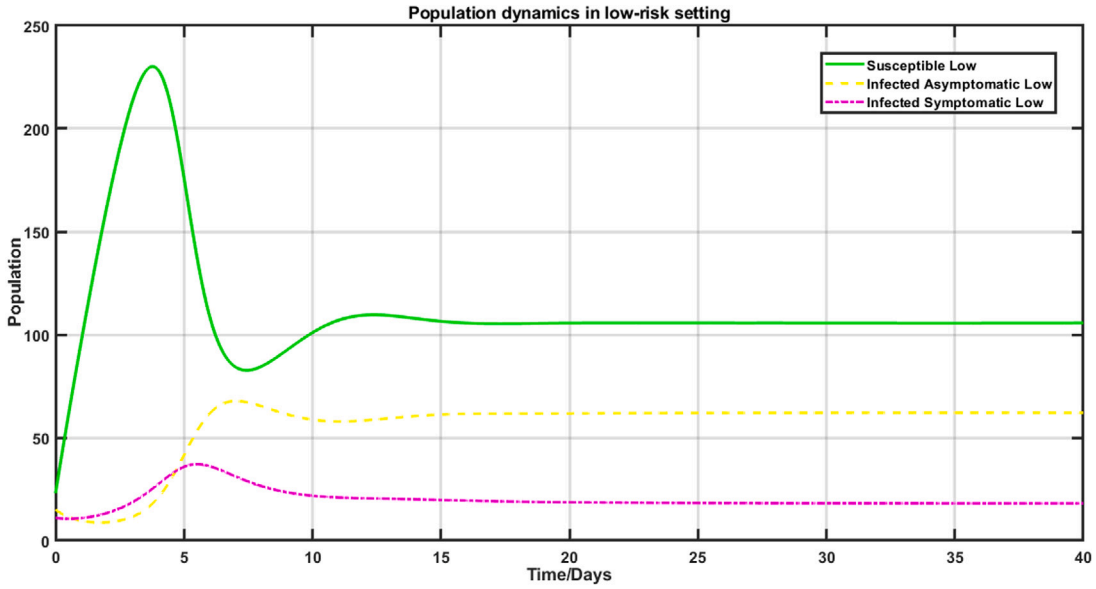

Fig. 5. Disease dynamics in a low-risk setting.

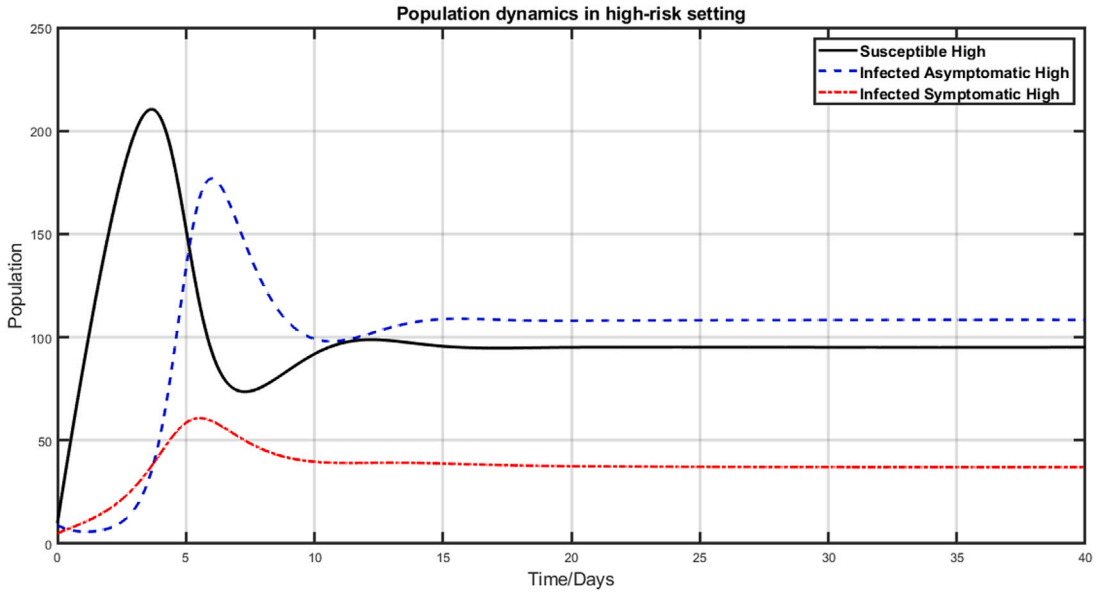

Fig. 6. Disease dynamics in a high-risk setting.

rises. Initially, the asymptomatic class is shallow and rises above the symptomatic as time increases due to the fact that most asymptomatic individuals are not treated or given any health support.

In general, we expect the disease to persist in low-risk settings due to the fact that there are no intervention measures incorporated into the model. Even though some models of Covid-19 suggest disease persistence in the presence of intervention measures (Lin et al., 2020; Asempapa et al., 2022). However, the infected populations are maintained at minimum manageable amounts.

Fig. 6 shows the simulation dynamics of Covid-19 in a high-risk setting. Generally, the trends for low and high-risk settings are the same but the numbers in high-risk are high as compared to the low-risk setting. In a high-risk setting, the infected asymptomatic population may rise above the susceptible population as time progresses but the symptomatic class remains low as the infected individuals are easily noticed quarantined, and given health care services. In a low-risk setting, the susceptible population is always higher than the susceptible population in a high-risk setting due to the fact that there are few positive cases in a low-risk area. The disease spreads more rapidly in a high-risk setting.

Again Fig. 6 shows the effects of parameters and factors driving the disease dynamics in high-risk settings. Since a high-risk setting was characterized by a high transmission rate the increase showed variable increases of infected asymptomatic and infected symptomatic in high-risk environments. As time progresses the disease dynamics stabilize to constant levels, and no shocks or jumps are observed after 15 days. In general, the disease persists in high-risk settings with a high transmission rate. However, we noted that the disease is not capable of infecting everyone or worse eradicating the whole population. It is upon the human population to adjust learning to live with the disease in these risk settings.

According to Fig. 7 shows the infected populations in both high-risk settings and low-risk settings. The infected population constitutes a sub-population with the major contributor in driving infections being asymptomatic in high-risk settings. These are individuals with the disease but show no symptoms and they are the main drivers of the

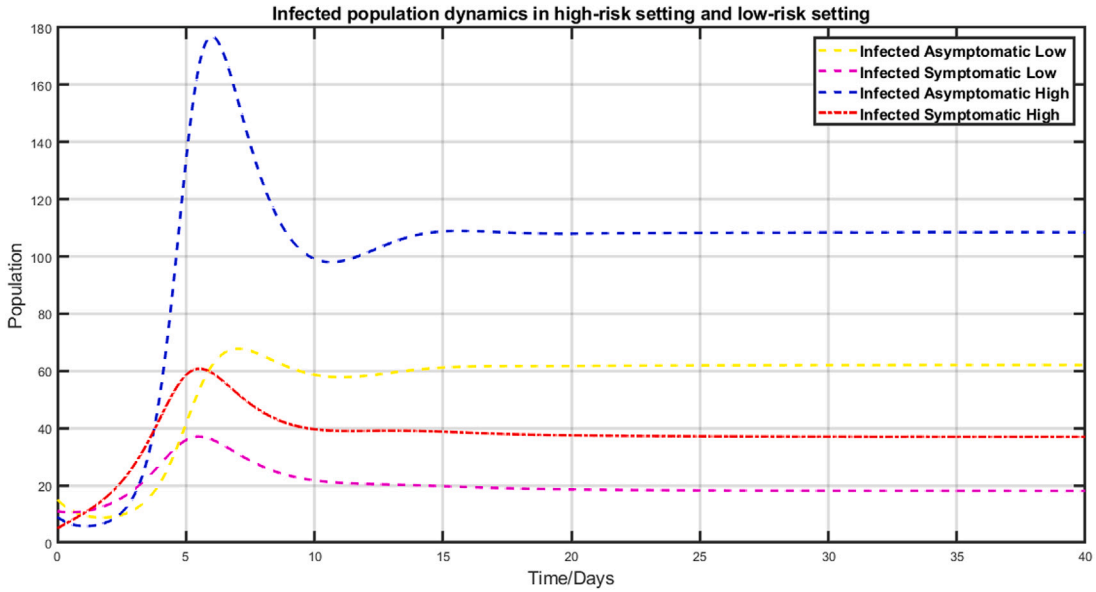

Fig. 7. Susceptible population dynamics.

disease as they can move and spread the disease to the population without being dictated. Also, the infected asymptomatic in low-risk settings plays an influential role in the spread of the disease in low-risk settings. Again, asymptomatic individuals can highly spread the disease since they can move and spread the disease within the population unnoticed. Hence, high testing rates were very important in controlling the disease in the presence of this type of people. Lastly, the two symptomatic classes played a minimum role in driving the dynamics of the disease in both settings.

4.2. Case 2: Switching between high and low-risk setting

In this section, we investigate the dynamics of Covid-19 with switching risk settings. In first case 1, the study considered high and low-risk settings while maintaining the same risk levels for different communities or populations. However, in practice risk levels of a certain community or population fluctuates and change with respect to time and space. This phenomenon is also supported by the seasonality nature of the disease and the notion of switching risk levels of setting seems to be more appropriate in the case of the Covid-19 model rather than maintaining the population risk settings at constant. Although holding risk levels constant seems okay for short time intervals it turns out to be unreliable for long time intervals.

Fig. 8 shows the population dynamics in high-risk setting switching to low-risk settings. The susceptible population raises rapidly to a maximum then drops and increases to a steady limit point. After the switch, the susceptible population increases fast reaching a horizontal limit. As for the infected asymptomatic population, no major population changes occur within the first few days of disease invasion but thereafter the asymptomatic population shoots to the maximum and steadily reduced to a point where it tails off to a horizontal limit. After the switch, the asymptomatic population decreases exponentially. Finally, the infected symptomatic population steadily increases to a maximum then immediately decays to some point and after the switch, the population slightly decreases exponentially.

Fig. 9 shows the population dynamics in low-risk setting switching to the high-risk setting. The susceptible population rapidly increases to a maximum and drops within a space of a week. Thereafter the susceptible population increased and steadily reached a limit. After the switch, the susceptible population slightly increased and leveled off in a doomed-shaped manner with minimum changes in the population levels before and after the switch. In terms, of the infected asymptomatic population delay was observed in response then after the delay followed an increase to the maximum before the graph tailed off to a horizontal limit. After the switch, the population steadily increased for about a week to reach an upper bound. Furthermore, the infected symptomatic population steadily increased and decayed in a belly-like curve. After the switch, the population increased steadily to reach an upper bound.

Fig. 10 shows the infected population dynamics with switching risk levels with a major noticeable change being the rapid decrease of the asymptomatic population from the high-risk setting switching to the low-risk setting. While the asymptomatic population rapidly increased by switching from low-risk setting to high-risk setting. On the other hand, minimum changes occurred with respect to the symptomatic populations. The symptomatic population from high-risk setting slightly decrease by switching to a low-risk setting and the symptomatic population from low-risk setting slightly increased by switching to high-risk setting.

5. Summary and recommendations

The progression and dynamics of the Covid-19 virus have presented socio-economic challenges to all populations across the globe. Many researchers have developed different mathematical models to understand the dynamics of the novel coronavirus disease Covid-19. Again, many vaccines have been developed to help cab the spread of the disease in both high-risk setting and low-risk setting. It is therefore pivotal to understand the propagation of the disease in different settings, especially with auto-switching characteristics either from low-risk setting to high-risk setting or from high-risk setting to low-risk setting. In this paper, we presented a mathematical model with switching risk settings. The switch from one setting to the other may be a result of changing disease management strategies or response factors due to the population reacting to the effects of the disease. Basically, the key changes were observed in the asymptomatic populations by the switch from one setting to the other setting. Whereas changes in the infected population were noted the changes observed were less pronounced as compared to those in asymptomatic populations.

In the article, a high-risk setting is characterized by a high infection rate, a high number of Covid-19 positive cases, and high numbers of asymptomatic individuals. The results of this research are useful as it aids in intervention strategies in different risk settings. The results

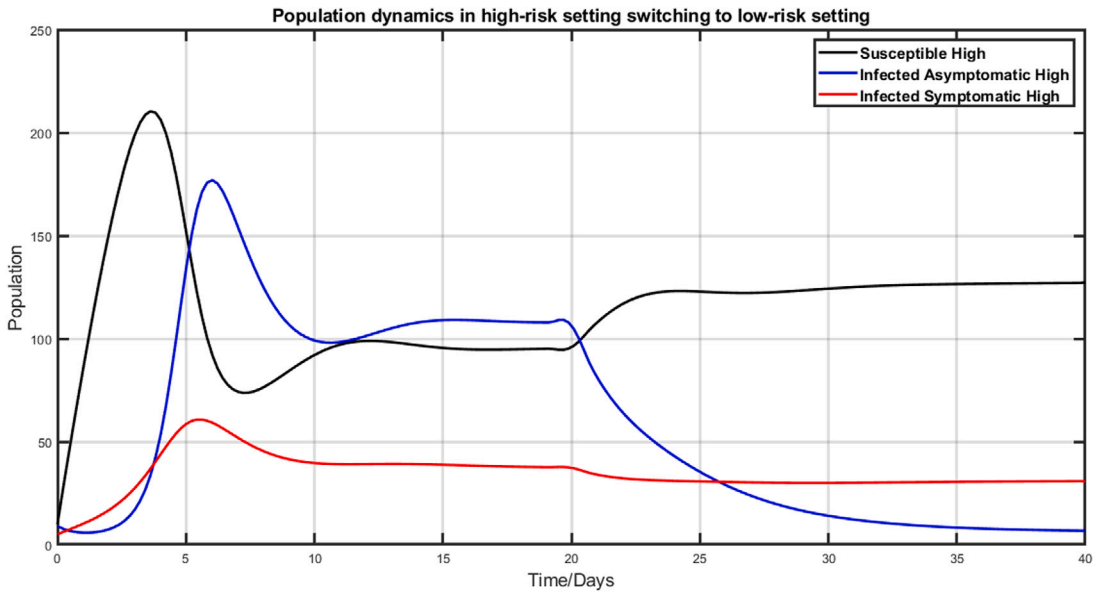

Fig. 8. Progression dynamics of infected population.

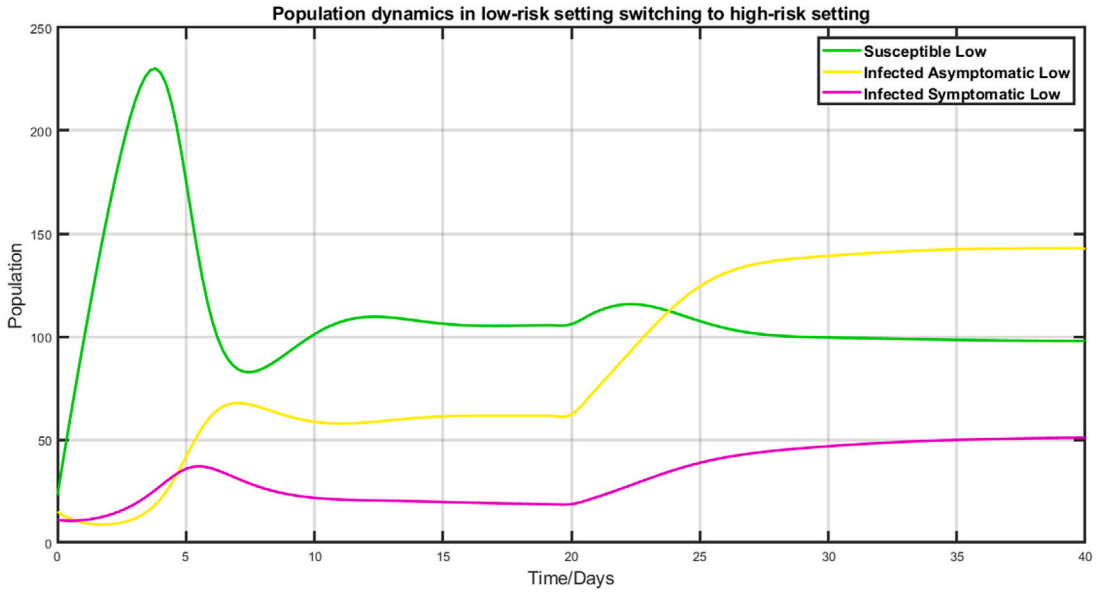

Fig. 9. Populations Progression dynamics of infected population.

indicate that more attention should be on high-risk settings as they increase the number of recorded cases and disease-induced death as well. Policy facilitators may also consider the discouraging movement of people from areas of low-risk settings to areas of high-risk settings. The results show that if the population was evenly distributed, high-risk areas would be minimized. More new Covid-19 variants are more likely to emerge as the virus mutates in high-risk settings. Hence, in low-risk settings, there are more infected asymptomatic individuals just like in high-risk settings. Policy facilitators ought to intensify testing in both settings as it will help determine the infected asymptomatic individuals. Infected asymptomatic individuals should also be quarantined as they can spread the disease unaware. Finally, we recommend that populations should continue immunization programs and also consider the loss of immunity to those who are fully vaccinated

CRediT authorship contribution statement

Meshach Ndlovu: Design of the model, Article writeup. **Mqhelewenkosi A. Mpofu:** Developed the mathematical model. **Rodwell G. Moyo:** Performed qualitative and quantitative analysis of the model.

Declaration of competing interest

The authors declare that they have no known competing financial interests or personal relationships that could have appeared to influence the work reported in this paper.

Data availability

Data will be made available on request.

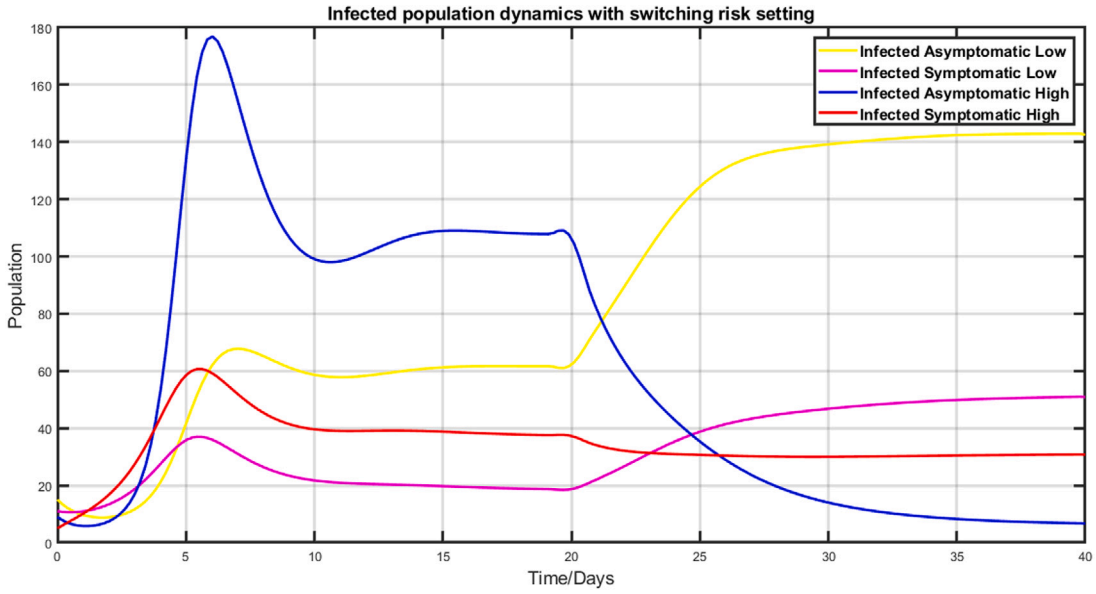

Fig. 10. Populations Progression dynamics of infected population1.

References

Anon, 2020. World health organization Coronavirus disease (COVID-19) pandemic. (Accessed 12 April 2020).

Anon, 2022. Zimbabwe National Statistics Agency 2022. https://zimbabwe.opendataforafrica.org/anjlptc/2022-population-housing-census-preliminary. (Accessed from 24 August 2022).

Asempapa, R., Oduro, B., Apenteng, O.O., Magagula, V.M., 2022. A COVID-19 mathematical model of at-risk populations with non-pharmaceutical preventive measures: The case of Brazil and South Africa. Infect. Dis. Model. (ISSN: 2468-0427) 7 (1), 45–61. http://dx.doi.org/10.1016/j.idm.2021.11.005.

Brindle, M.E., Gawande, A., 2020. Managing COVID-19 in surgical systems. Ann. Surg. 272 (1), e1–e2. http://dx.doi.org/10.1590/0100-6991e-20202536.

Dzinamarira, Tafadzwa, Nachipo, Brian, Phiri, Bright, Musuka, Godfrey, 2021. COVID-19 vaccine roll-out in South Africa and Zimbabwe: Urgent need to address community preparedness. Fears Hesitancy Vaccines 9 (3), 250. http://dx.doi.org/10.3390/vaccines9030250.

Galbadage, T., Peterson, B.M., 2020. Coronavirus COVID-19 SARS-CoV-2 droplet viral transmission pandemic outbreak epidemic formite indirect transmission aerosol. Front. Public Health 8, 2296–2565.

Garira, W., 2018. A primer on multiscale modelling of infectious disease systems. Infect. Dis. Model. (ISSN: 2468-0427) 3, 176–191. http://dx.doi.org/10.1016/j.idm.2018.09.005.

Garira, W., Mathebula, D., Netshikweta, R., 2014. A mathematical modelling framework for linked within-host and between-host dynamics for infections with free-living pathogens in the environment. Math. Biosci. (ISSN: 0025-5564) 256, 58–78. http://dx.doi.org/10.1016/j.mbs.2014.08.004.

He, D., Dushoff, J., Day, T., Ma, J., Earn, D.J., 2013. Inferring the causes of the three waves of the 1918 influenza pandemic in England and Wales. Proc. R. Soc. B 280 (1766), 20131345.

Kumar, I.S., 2020. Symptoms, prophylaxis and social responsibilities during COVID-19 outbreak. Eur. J. Biomed. 7, 2349–8870, http://www.ejbps.com/.

Li, Q., Med, M., Guan, X.H., 2020. Early transmission dynamics in Wuhan, China, of novel Coronavirus–infected pneumonia. N. Engl. J. Med. http://dx.doi.org/10.1056/NEJMoa2001316.

Lin, Q., Zhao, S., Gao, D., 2020. A conceptual model for the outbreak of Coronavirus disease 2019 (COVID-19) in Wuhan, China with individual reaction and governmental action. Int. J. Infect. Dis. 93, 211–216. http://dx.doi.org/10.1016/j.ijid.2020.02.058.

Mackworth-Young, C.R., Chingono, R., Mavodza, C., McHugh, G., Tembo, M., Chikwari, C.D., Weiss, H.A., Rusakaniko, S., Ruzario, S., Bernays, S., Ferrand, R.A., 2021. Community perspectives on the COVID-19 response, Zimbabwe. Bull. World Health Organ. 99 (2), 85–91. http://dx.doi.org/10.2471/BLT.20.260224.

Murewanhema, G., Makurumidze, R., 2020. Essential health services delivery in Zimbabwe during the COVID-19 pandemic: Perspectives and recommendations. Pan African Med. J. 35 (Suppl 2), 143. http://dx.doi.org/10.11604/pamj.supp.2020.35.143.25367.

Mushayabasa, S., Ngarakana-Gwasira, E.T., Mushanyu, J., 2020. On the role of governmental action and individual reaction on COVID-19 dynamics in South Africa: A mathematical modelling study. Inform. Med. Unlocked 20, 100387. http://dx.doi.org/10.1016/j.imu.2020.100387.

Mushayi, C., Nyabadza, F., Chigidi, E., Mataramvura, H., Pfavayi, L., Rusakaniko, S., Sibanda, E.N., 2021. A mathematical model for the prediction of the prevalence of allergies in Zimbabwe. World Allergy Organ. J. 14 (7), 100555. http://dx.doi.org/10.1016/j.waojou.2021.100555, 1939-4551.

Ndlovu, M., Moyo, R., Mpofu, M., 2022. Modelling COVID-19 infection with seasonality in Zimbabwe. Phys. Chem. Earth (2002) 127, 103167. http://dx.doi.org/10.1016/j.pce.2022.103167.

Rali, A.S., Sauer, A.J., 2020. COVID-19 pandemic and cardiovascular disease. US Cardiol. Rev. 14, e01. http://dx.doi.org/10.15420/usc.2020.14.

Riou, J., Althaus, C.L., 2020. Pattern of early human-to-human transmission of Wuhan 2019 novel Coronavirus (2019-nCoV), 2019 to 2020. Euro Surveill. 25 (4), 2000058. http://dx.doi.org/10.2807/1560-7917.ES.2021.25.4.2000058, published correction appears in Euro Surveill. 2020 Feb;25(7).

Volpicelli, G., Gargani, L., 2020. Sonographic signs and patterns of COVID-19 pneumonia. Ultrasound J. 12 (1), 22. http://dx.doi.org/10.1186/s13089-020-00171-w.

Weiss, H.H., 2013. The SIR model and the foundations of public health. Mater. Math. 0001–0017.

Xiang, Y.T., Li, W., Zhang, Q., Jin, Y., Rao, W.W., Zeng, L.N., Lok, G., Chow, I., Cheung, T., Hall, B.J., 2020. Timely research papers about COVID-19 in China. Lancet (London, England) 395 (10225), 684–685. http://dx.doi.org/10.1016/S0140-6736(20)30375-5.

Zhong, L., Mu, L., Li, J., Wang, J., Yin, Z., Liu, D., 2021. Outbreak in the mainland China based on simple mathematical model. IEEE Access 8, 51761–51769.

Zhou, T., Liu, Q., Yang, Z., 2020. Early prediction of the 2019 novel Coronavirus preliminary prediction of the basic reproduction number of the Wuhan novel Coronavirus 2019-nCoV. Evid. Base Med. 13 (1), 3–7. http://dx.doi.org/10.1111/jebm.12376.

Zhu, N., Zhang, D., Wang, W., 2020. A novel Coronavirus from patients with pneumonia in China, 2019. N. Engl. J. Med. http://dx.doi.org/10.1056/NEJMoa2001017, PMC free article PubMed CrossRef Google Scholar.